



Infrared photobiomodulation (PBM) therapy improves glucose metabolism and intracellular insulin pathway in adipose tissue of high-fat fed mice

Gabriela Silva¹ · Cleber Ferraresi^{2,3} · Rodrigo Teixeira de Almeida¹ · Mariana Lopes Motta¹ · Thiago Paixão¹ · Vinicius Oliveira Ottone¹ · Ivana Alice Fonseca¹ · Murilo Xavier Oliveira⁴ · Etel Rocha-Vieira¹ · Marco Fabrício Dias-Peixoto¹ · Elizabeth Adriana Esteves¹ · Cândido Celso Coimbra^{1,5} · Fabiano Trigueiro Amorim^{1,6} · Flávio de Castro Magalhães¹

Received: 25 July 2017 / Accepted: 29 November 2017 / Published online: 15 December 2017
© Springer-Verlag London Ltd., part of Springer Nature 2017

Abstract

Obesity represents a continuously growing global epidemic and is associated with the development of type 2 diabetes mellitus. The etiology of type 2 diabetes is related to the resistance of insulin-sensitive tissues to its action leading to impaired blood glucose regulation. Photobiomodulation (PBM) therapy might be a non-pharmacological, non-invasive strategy to improve insulin resistance. It has been reported that PBM therapy in combination with physical exercise reduces insulin resistance. Therefore, the aim of this study was to investigate the effects of PBM therapy on insulin resistance in obese mice. Male Swiss albino mice received low-fat control diet ($n = 16$, LFC) or high-fat diet ($n = 18$, HFD) for 12 weeks. From 9th to 12th week, the mice received PBM therapy (LASER) or Sham (light off) treatment and were allocated into four groups: LFC Sham ($n = 8$), LFC PBM ($n = 8$), HFD Sham ($n = 9$), and HFD PBM ($n = 9$). The PBM therapy was applied in five locations: to the left and right quadriceps muscle, upper limbs and center of the abdomen, during 40 s at each point, once a day, 5 days a week, for 4 weeks (780 nm, 250 mW/cm², 10 J/cm², 0.4 J per site; 2 J total dose per day). Insulin signaling pathway was evaluated in the epididymal adipose tissue. PBM therapy improved glucose tolerance and phosphorylation of Akt (Ser473) and reversed the HFD-induced reduction of GLUT4 content and phosphorylation of AS160 (Ser588). Also, PBM therapy reversed the increased area of epididymal and mesenteric adipocytes. The results showed that chronic PBM therapy improved parameters related to obesity and insulin resistance in HFD-induced obesity in mice.

Keywords Low-level laser therapy · Insulin resistance · Glucose intolerance · Type 2 diabetes mellitus · Insulin signaling

Introduction

Obesity is a growing global public health problem and generally is associated with the development of non-communicable chronic diseases such as type 2 diabetes (T2D) [1]. The

etiology of T2D is characterized by insulin resistance in tissues sensitive to the action of this hormone, including the adipose tissue [2]. Moreover, previous studies already have shown that obesity is related to an increased morbidity and mortality through the development of insulin resistance [3].

✉ Flávio de Castro Magalhães
magalhaesufing@gmail.com

¹ Programa Multicêntrico de Pós-Graduação em Ciências Fisiológicas, Faculdade de Ciências Básicas e da Saúde, Universidade Federal dos Vales do Jequitinhonha e Mucuri, Diamantina, Brazil

² Post-graduation Program in Physical Therapy in Functional Health, Physical Therapy Department, Universidade do Sagrado Coração, São Paulo, Brazil

³ Post-Graduation Program in Biomedical Engineering, Universidade Brasil, São Paulo, Brazil

⁴ Programa de Pós-Graduação em Reabilitação e Desempenho Funcional, Physiotherapy Department, Faculdade de Ciências Básicas e da Saúde, Universidade Federal dos Vales do Jequitinhonha e Mucuri, Diamantina, Brazil

⁵ Endocrinology Laboratory, Biological Sciences Institute, Federal University of Minas Gerais, Belo Horizonte, Brazil

⁶ University of New Mexico, Albuquerque, NM, USA

The mechanism of obesity-related insulin resistance has not been fully elucidated, but evidences suggest that the accumulation of intracellular fat followed by increases in fatty acid metabolites play a role in the development of insulin resistance [4]. Increment in intracellular fatty acid content leads to ectopic fat accumulation in skeletal muscle and adipose and liver tissues, resulting in accumulation of fatty acid intermediates. The fatty acid intermediates lead to increase in pro-inflammatory pathways [5] and inflammatory cytokine release [6] that activate stress kinases [7] leading to an impaired insulin signaling [8].

It is demonstrated that chronic activation of the stress kinase c-Jun NH₂-terminal kinase (JNK) can induce insulin resistance by affecting insulin signaling pathway and GLUT4 expression in 3T3-L1 adipocytes [9]. It has been also demonstrated that in diet-induced obesity mice, JNK is over activated, affecting insulin signaling pathway, while JNK knockout mice are protected from diet-induced obesity and insulin resistance [10]. Therefore, JNK is considered a central stress kinase involved in insulin resistance in obesity.

Photobiomodulation (PBM) therapy consists in a non-invasive therapeutic intervention, using a low-intensity light source [11], such as light amplification by stimulated emission of radiation (LASER) or light-emitting diode (LED). PBM can reduce cellular stress by stimulating anti-inflammatory enzyme activity [12] and reducing the activation of pro-inflammatory pathways [13]. There is evidence that PBM combined with physical exercise was more effective in reducing insulin resistance than exercise alone in obese women [14]. However, the isolated effects of PBM on insulin resistance and insulin signaling pathway, as well as on JNK activation, have not been studied. Therefore, the aim of the present study was to investigate the effects of PBM on insulin resistance, intracellular insulin pathway, and JNK activation in high-fat fed mice.

Materials and methods

Animal model

Thirty-four, eight-week-old, male Swiss albino mice were fed with standard chow for 2 weeks before starting either a low-fat diet (LFD) or a high-fat diet (HFD). Mice were housed at 8 animals per cage, kept on a 12-h light 12-h dark cycle with room temperature set at 22 ± 2 °C, with free access to water and chow. All procedures followed the National Council of Animal Experimentation (Brazil) and were approved by the local Ethics Committee on Animal Use under the number 028/2014.

Experimental design

Mice were randomly allocated into two equal groups and fed with LFD or HFD for 12 weeks, starting at 10th week of age. Mice were adapted to handling for PBM therapy for 5 days during the week preceding the beginning of the actual protocol. After 8 weeks of diet, LFD and HFD were further allocated equally into Sham (LFD SHAM, $n = 8$, and HFD SHAM, $n = 9$) or photobiomodulation (LFD PBM, $n = 8$, and HFD PBM, $n = 9$). From the 9th week of diet to the end of the 12th week, the mice were treated 5 days/week with PBM or SHAM, totaling 20 sessions. At the end of the 8th and 12th weeks, intraperitoneal glucose tolerance tests (ipGTT) were performed. Forty-eight hours after the last session of treatment (SHAM or PBM), the mice were euthanized and tissues were harvested for histological and protein blot analysis. The experimental design is shown in Fig. 1.

Diet

Diet compositions were based on Research Diet open formula of purified diets (<http://www.researchdiets.com/>). The LFD was based on D12450J formula (calories derived from protein, carbohydrate, and fat were 20, 70, and 10%, respectively), and the HFD was based on D12492 formula (calories derived from protein, carbohydrate, and fat were 20, 20, and 60%, respectively). The diet compositions are presented in Table 1. For an estimation of diet intake, chow was weighed three times a week and the difference between offer and left over was divided by the number of animals in the cage. The mice were weighed once a week.

Photobiomodulation therapy

PBM therapy was applied using a commercially available laser device (MMOptics LTDA., Twin Flex III Evolution, São Carlos, Brazil). PBM parameters are shown in Table 2. For the light irradiation in SHAM or PBM groups, mice were held by their back skin, and the laser probe was positioned in contact with the quadriceps femoris muscles bilaterally, upper hind limbs, and center of the abdomen, totaling five sites of irradiation. SHAM-treated mice were handled in the same manner as the PBM-treated mice, but the LASER probe was switched off.

Intraperitoneal glucose tolerance test

For assessment of glucose tolerance, ipGTT was performed at the end of the 8th and 12th weeks, 24 h after the last PBM session. Mice were fasted for 6 h, and 1 mg of dextrose per gram of body weight (diluted in saline—20% w/v) was injected intraperitoneally. Blood glucose was measured prior to (0 min) and after dextrose injection at 15, 30, 60, 120, and

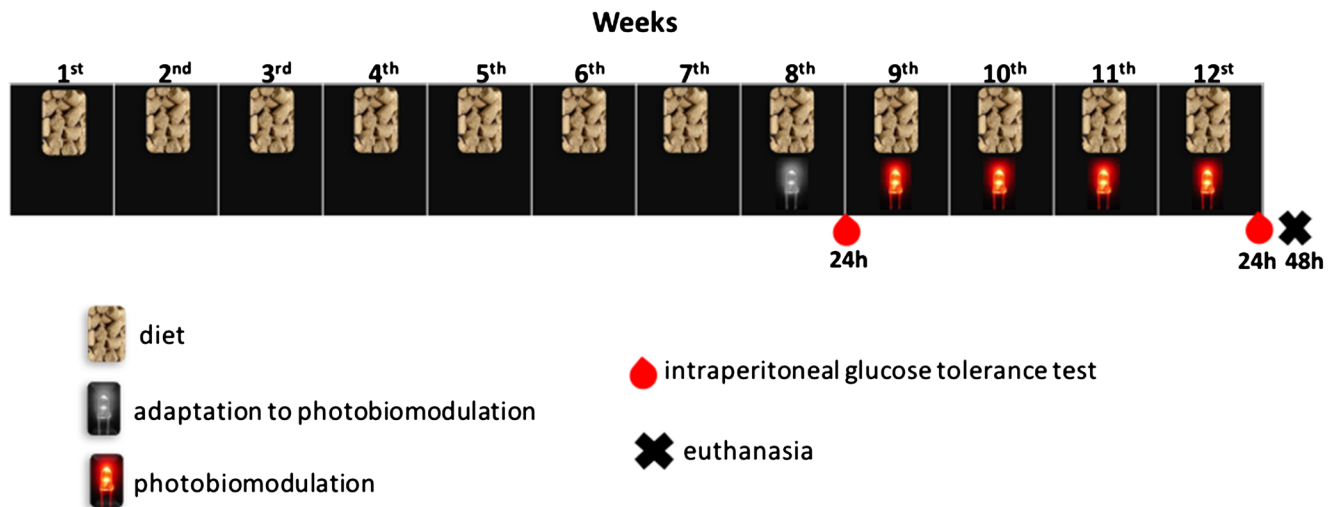


Fig. 1 Experimental design

180 min. Blood glucose was measured with a glucose meter (Accu-Chek Performa Nano, Roche, Rio de Janeiro, Brazil) by tail puncture.

Euthanasia

Forty-eight hours after the last SHAM or PBM session, mice were anesthetized with an intraperitoneal injection of 60 mg/kg ketamine and 10 mg/kg xylazine. After complete loss of response, 200 μ L of blood was drawn from the mouse's tail for analysis. Insulin (\sim 300 μ L; 10 U/kg; Humulin R–Lilly, Indianapolis, USA) or saline (\sim 300 μ L) was also intraperitoneally injected for activation of insulin pathway. Ten minutes after the injection, the mice were euthanized by cervical dislocation.

Table 1 Diet compositions

Ingredient	Quantity (g)	
	Low-fat diet (LFD)	High-fat diet (HFD)
Protein (casein)	200.0	200.0
Maltodextrin	125.0	125.0
Sucrose	68.8	68.8
Cellulose	50.0	50.0
Soybean oil	25.0	25.0
Lard	20.0	245.0
Mineral mix	35.0	35.0
Vitamin mix	10.0	10.0
L-cystine	3.0	3.0
Choline bitartrate	2.0	2.0
Corn starch	506.2	0.0
Total	1045	763.8
kcal/g	3.85	5.24

Blood analysis

Blood samples were allowed to clot at 37 °C via water bath for 30 min and the serum was separated by centrifugation (3000 \times g, 20 min, 4 °C). The serum aliquots were stored at -20 °C until analysis. Total cholesterol, triglyceride, and glucose were measured with commercially available colorimetric kits (Labtest, Lagoa Santa, Brasil). Insulin was assessed by radioimmunoassay (Insulin RIA kit, Millipore, cat. # RI-13K, St. Charles, Missouri, USA) following manufactures' guidelines.

Insulin resistance was assessed by the homeostatic model assessment of insulin resistance (HOMA-IR) following Matthews et al. [15]: $\text{HOMA-IR} = \text{fasting glycaemia (mmol)} \times \text{fasting insulin } (\mu\text{U/mL}) / 22.5$.

Table 2 Optical parameters of laser treatment. SHAM groups were handled in the same manner (device switched off) with the same time of treatment

Variables	Characteristics
Wavelength	780 nm
Pulse frequency	Continuous
Optical output	10 mW
LASER spot size	0.04 cm ²
Power density	250 mW/cm ²
Energy delivered per site	0.4 J
Energy density	10 J/cm ²
Treatment time (per site)	40 s
Number of irradiation sites	5
Total irradiation time	200 s
Total energy delivered per animal	2 J
Application mode	Skin contact

Adipose tissue harvesting

Epididymal, retroperitoneal, and mesenteric adipose fat pads were harvested, cleaned in cold saline, and dried in filter paper and weighed. The tissues were separated in aliquots for Western blot analysis (snap frozen in liquid nitrogen and stored at $-80\text{ }^{\circ}\text{C}$) and histological analysis.

Histological analysis

The tissue samples were fixed in buffered formalin (10%) for 24 h and were paraffin-embedded (Merck, Darmstadt, Germany) and subjected to histological cuts ($4\text{ }\mu\text{m}$) before being routinely processed for histology and hematoxylin-eosin staining. Adipocyte area was assessed using ImageJ software (ImageJ 1.49, Wayne Rasband, National Institutes of Health, USA). To assess adipocyte area, images were captured using a $100\times$ increase in magnification, and three fields per sample were randomly chosen by one of the co-authors blinded for the groups. Only adipocytes that had clear border were considered for assessing cell area. Approximately 100 cells per animal were measured.

Protein analysis

Protein content and phosphorylation status were assessed by Western blot, as previously described [16, 17]. Briefly, epididymal fat pad samples ($\sim 50\text{ mg}$) were homogenized in cold lysis buffer (1% Triton $\times 100$; 100 mM Tris pH 8.0, 20% glycerol, 0.2 mM EDTA) containing protease inhibitor cocktail (Complete Protease Inhibitor Cocktail, Roche, Germany) and phosphatase inhibitor cocktail (Phosphatase Inhibitor Cocktail PhosStop, Roche, Germany). The lysates were centrifuged at $12,000\times g$ for 5 min at $4\text{ }^{\circ}\text{C}$, and supernatant was collected and subjected to another centrifugation (using the same parameters) for proper fat separation. Protein concentration was assessed by Bradford method [18], using bovine serum albumin (BSA) as standard.

The samples were diluted in sample buffer and heated at $95\text{ }^{\circ}\text{C}$ for 5 min. Approximately 30 mg of total protein was fractioned in polyacrylamide gels (8–12%) using SDS-PAGE technique (Bio-Rad, Mini-Protean Tetra Cell Systems, Hercules, USA) before being transferred to PVDF membranes (Bio-Rad, Power Pac Basic Power Supply, Hercules, USA). To check for transference efficiency, membranes were Ponceau stained.

The membranes were blocked by incubation with 10% BSA in TBS-tween buffer for 1 h at room temperature. Then, membranes were in primary antibody (1:1000, 1% BSA, TBS-tween), under agitation at $4\text{ }^{\circ}\text{C}$, overnight, and after that, they were incubated in HRP-conjugated secondary antibody (1:5000, 1% BSA, TBS-tween) for 2 h at room temperature. Primary antibodies used were phospho-Akt (Ser

473), total Akt, phospho-AS160 (Thr642), Phospho-AS160 (Ser588), Glut4, Phospho-SAPK/JNK (Thr183/Tyr185), β -Actin (all from Cell Signaling). Secondary antibodies were anti-rabbit IgG and anti-mouse IgG (both from Cell Signaling).

The membranes were incubated with Luminata Forte (Merck Millipore, Darmstadt, Germany) for 3 min protected from light, and bands were visualized by photodocumentation (Loccus Biotecnologia, Cotia, Brazil) and quantified by ImageJ software (ImageJ 1.49, Wayne Rasband, National Institutes of Health, USA).

Statistical analysis

The software Statistica was used for statistical analysis (v10.0, StatSoft, Inc). Data normality was verified by Shapiro-Wilk test, and two-way (diet versus treatment) or three-way (diet versus treatment versus insulin stimulation) analysis of variance (ANOVA) was used to evaluate the difference between treatments. When a significant *F* value was detected, Tukey post hoc test was used. Significance was set at 5% and data is shown as mean \pm SEM.

Results

Diet intake

Table 3 presents the results for dietary intake during the 12-week diet and PBM therapy. Food intake in grams was lower in the HFD groups (diet effect $p < 0.0001$), but there was no PBM interaction ($p = 0.45$) or diet and PBM interaction ($p = 0.32$). Furthermore, no main effects for week (1–8 versus 9–12 weeks, $p = 0.61$), week versus diet ($p = 0.85$), week versus PBM ($p = 0.73$), or week versus diet versus PBM ($p = 0.53$) were observed. On the other hand, when caloric intake was calculated, there was no effect for PBM ($p = 0.57$), diet ($p = 0.55$), PBM versus diet ($p = 0.39$), week ($p = 0.67$), week versus PBM ($p = 0.90$), week versus diet ($p = 0.80$), week versus PBM versus diet ($p = 0.60$), indicating that although the groups differed in diet intake, the caloric intake was not different.

Body mass, growth parameters

Table 4 reports results for body mass and growth parameters during the 12 weeks of intervention. In the beginning of the first week, groups did not differ in body mass ($p = 0.97$), but both groups increased their body mass by the end of the eighth week ($p < 0.0001$), although HFD groups were significantly heavier than LFD groups in the 8th ($p = 0.00008$) and 12th ($p < 0.0001$) weeks. Body mass was not different within groups in weeks 8 and 12 ($p = 0.76$). Table 4 also shows that there was

Table 3 Effects of 8 weeks of diet type intervention and 4 weeks of diet plus photobiomodulation on diet and caloric intake

	LFD Sham	LFD PBM	HFD Sham	HFD PBM
Diet intake 1–8 weeks (g/day)	5.8 ± 0.4	5.6 ± 0.5	4.2 ± 0.7*	4.2 ± 0.4*
Diet intake 9–12 weeks (g/day)	5.8 ± 1.0	5.4 ± 0.9	4.1 ± 0.7*	4.2 ± 0.5*
Caloric intake 1–8 weeks (kcal/day)	22.1 ± 1.7	21.5 ± 1.9	22.1 ± 3.4	22.1 ± 2.0
Caloric intake 9–12 weeks (kcal/day)	22.2 ± 3.8	21.0 ± 3.3	21.5 ± 3.4	22.2 ± 2.8

LFD low-fat diet, HFD high-fat diet. SHAM: PBM photobiomodulation

* $p < 0.05$ vs LFD

no effect of diet ($p = 0.67$), PBM (0.29), or diet versus PBM interaction ($p = 0.81$) on nasal-anal length, nor effect of diet ($p = 0.73$), PBM ($p = 0.96$), or diet versus PBM interaction ($p = 0.44$) on tibia length, indicating that these interventions did not differentially affect mice growth.

Fat pad mass and adipocyte hypertrophy

There was main effect interaction ($p = 0.03$) for diet versus PBM for epididymal fat pad mass. Post hoc analysis showed that HFD Sham group had heavier fat mass ($p = 0.009$) compared with LFD Sham and HFD PBM had significantly lighter fat mass ($p = 0.02$) compared with HFD Sham (Fig. 2a). For epididymal adipocyte hypertrophy, there was diet ($p = 0.01$) and PBM interaction ($p = 0.005$). Post hoc analysis showed that HFD Sham group had larger adipocytes compared with LFD Sham ($p = 0.0003$), and HFD PBM group had smaller adipocytes than HFD Sham ($p = 0.002$) (Fig. 2b). Figure 2c brings representative micrographs of the epididymal adipocytes.

HFD induced 300% increases in retroperitoneal fat pad mass (Fig. 2d, diet main effect $p = 0.00007$) and 50% of increases in retroperitoneal adipocyte hypertrophy (Fig. 2e, diet main effect $p = 0.03$). There was no PBM interaction ($p = 0.70$) or interaction for retroperitoneal fat pad mass ($p = 0.84$), as well as no PBM ($p = 0.52$) or retroperitoneal adipocyte hypertrophy interaction ($p = 0.88$). Figure 2f presents representative micrographs of the retroperitoneal adipocyte.

HFD induced an increase in mesenteric fat pad mass (diet main effect $p = 0.0001$); however, no difference

was observed after PBM therapy (Fig. 2g, PBM main effect $p = 0.68$) as well as no main effect interaction was observed ($p = 0.41$). There was a main effect interaction for mesenteric adipocyte hypertrophy ($p = 0.01$). Post hoc analysis revealed that HFD SHAM group had more hypertrophied mesenteric adipocytes compared with the LFD SHAM group ($p = 0.034$, Fig. 2h), and PBM therapy reduced mesenteric adipocyte hypertrophy in HFD compared with the HFD SHAM group ($p = 0.031$). Figure 2i presents representative micrographs of the mesenteric adipocyte.

Serum lipid profile

Serum triglyceride concentration was not affected by diet (diet main effect $p = 0.32$) or PBM therapy (PBM main effect $p = 0.63$), and thus, there was no main effect interaction ($p = 0.81$) (Fig. 3a). The total serum cholesterol was not affected by diet (diet main effect $p = 0.39$), but there was a PBM main effect ($p = 0.047$). Post hoc revealed that PBM reduced total serum cholesterol ($p = 0.043$), regardless of diet treatment (Fig. 3b).

Glucose metabolism

Figure 4 presents the results for glucose metabolism after 8 (diet only) and 12 weeks (diet plus 4 weeks of PBM) of intervention. Eight weeks of HFD led to hyperglycemia (diet main effect $p < 0.00001$, Fig. 4a), glucose intolerance (diet main effect $p < 0.00001$, Fig. 4b), and greater area under the curve

Table 4 Effects of 8 weeks of diet type intervention and 4 weeks of diet plus PBM on mice growth parameters

	LFD Sham	LFD PBM	HFD Sham	HFD PBM
Body mass 1st week (g)	41.4 ± 1.7	40.9 ± 3.8	40.0 ± 1.5	40.2 ± 1.5
Body mass 8th week (g)	50.6 ± 3.5	50.3 ± 2.9	58.1 ± 5.6*	58.3 ± 5.9*
Body mass 12th week (g)	49.6 ± 4.2	48.5 ± 4.4	58.8 ± 6.7*	58.6 ± 7.7*
Nasal-anal length (cm)	11.6 ± 0.5	11.9 ± 0.7	11.8 ± 0.2	11.9 ± 0.4
Tibia length (cm)	1.96 ± 0.06	1.97 ± 0.04	1.97 ± 0.06	1.95 ± 0.08

LFD low-fat diet, HFD high-fat diet. SHAM: PBM photobiomodulation

* $p < 0.05$ for diet effect

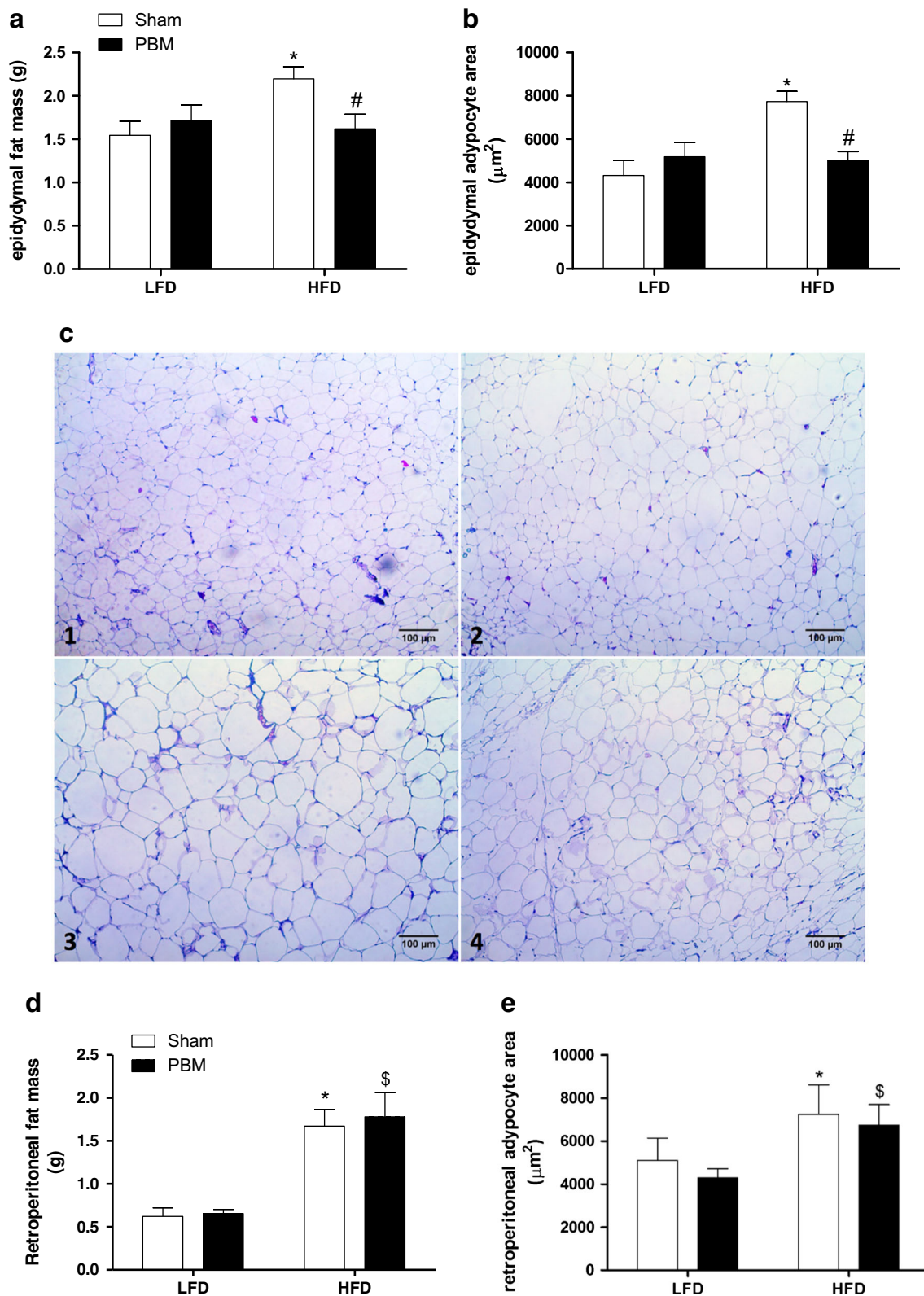


Fig. 2 Effect of photobiomodulation (PBM) on **a** epididymal fat mass, **b** epididymal adipocyte area, **d** retroperitoneal fat mass, **e** retroperitoneal adipocyte area, **g** mesenteric fat mass, **h** mesenteric adipocyte area and in low-fat diet (LFD)-fed and high-fat diet (HFD)-fed mice. In **c**, **f**, **i**,

representative histological images of (1) LFD Sham, (2) LFD PBM, (3) HFD Sham, and (4) HFD PBM are shown. * $p < 0.05$ versus LFD Sham; # $p < 0.05$ versus HFD Sham

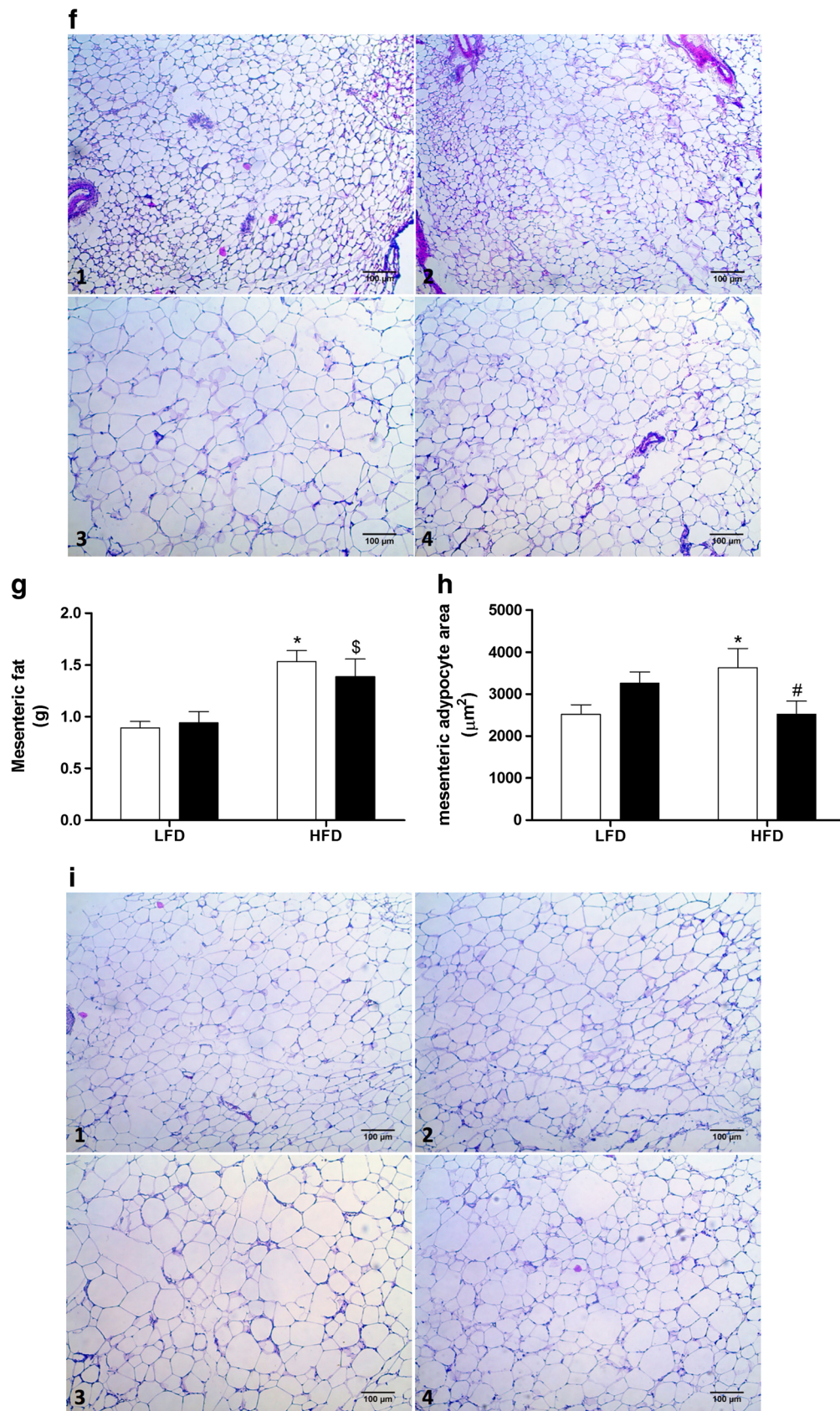


Fig. 2 (continued.)

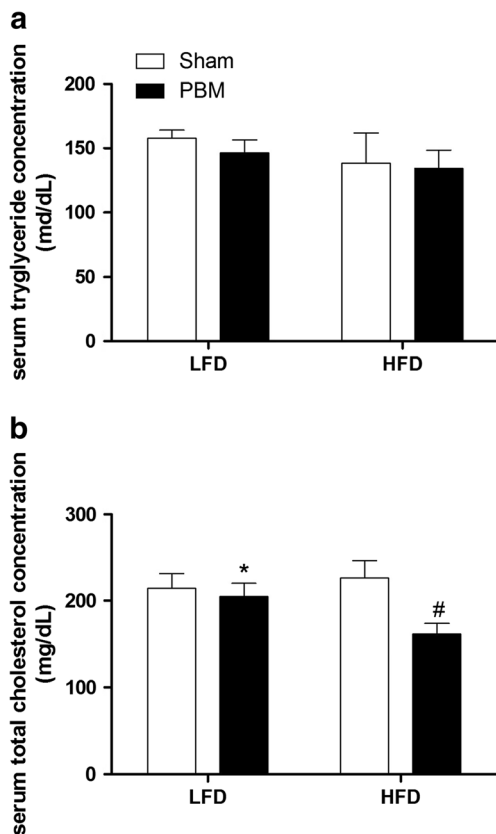


Fig. 3 Effect of photobiomodulation (PBM) on **a** serum triglyceride concentration and **b** serum total cholesterol concentration in low-fat diet (LFD)-fed and high-fat diet (HFD)-fed mice. * $p < 0.05$ versus LFD Sham; # $p < 0.05$ versus HFD Sham

(diet effect $p < 0.00001$, Fig. 4c). These data indicate that 8 weeks of HFD intervention led to disturbances in glucose metabolism.

After PBM concomitant to diet treatment, HFD groups maintained higher fasting glycemia ($p < 0.00001$), but there was no main effect interaction ($p = 0.22$), nor PBM interaction ($p = 0.31$) (Fig. 4d). In response to ipGTT, HFD groups showed higher glucose intolerance (diet main effect $p < 0.00001$); however, there was main effect interaction ($p = 0.01$) with PBM interaction ($p = 0.019$). Post hoc analysis showed improved glucose intolerance in HFD PBM (Fig. 4e). Furthermore, analysis revealed a diet effect ($p < 0.00001$) for area under the curve after PBM concomitant with diet and main effect interaction ($p = 0.04$). Post hoc analysis showed that HFD groups, regardless of PBM treatment, had greater area under the curve compared with their LFD controls, although HFD PBM group had lower ($p = 0.005$) area under the curve compared with HFD Sham (Fig. 4f). After the PBM intervention, there was a diet ($p < 0.00001$), but no PBM ($p = 0.53$) as well as main effect interaction ($p = 0.54$) for serum insulin concentration (Fig. 4g). Similar results were observed for HOMA-IR (diet main effect $p < 0.00001$; PBM effect $p = 0.57$; interaction main effect $p = 0.81$, Fig. 4h).

These data indicate that PBM concomitant with HFD was able to attenuate many of the disturbances in glucose metabolism.

Protein analysis

The results of protein analysis by Western blot are shown in Fig. 5a–e. There was main effect interaction for diet versus PBM versus insulin treatment for AKT activation ($p = 0.003$). Post hoc analysis showed that in LFD Sham, LFD PBM, and HFD PBM groups (all $p < 0.05$), insulin had higher AKT activation. On the other hand, only in HFD Sham group, insulin did not increase AKT activation ($p = 0.29$) (Fig. 5b). Akt substrate, AS160 phosphorylation, was assessed at two sites. Similar results for insulin-induced AS160 ser588 phosphorylation were observed where only in HFD Sham group, insulin did not increase AS160 ser588 ($p = 0.64$), whereas in all other groups, insulin could phosphorylate AS160 ser588 ($p < 0.05$ for all) (Fig. 5c). For AS160 thr642, insulin stimulated AKT only in LFD Sham ($p < 0.00001$), and this response was not observed in the other groups (LFD PBM, $p = 0.10$; HFD Sham, $p = 0.09$; HFD PBM, $p = 0.27$) (Fig. 5d). AS160 targets GLUT4 vesicles and Akt-mediated phosphorylation of AS160 leads to GLUT4 translocation to sarcolemma membrane and glucose uptake. The insulin stimulation led to increase GLUT4 content in LFD groups (both $p < 0.001$), which was completely inhibited in the HFD SHAM group ($p = 0.82$). However, PBM therapy prevented HFD-induced decrease in GLUT4 content ($p = 0.00002$) (Fig. 5e). Figure 5a presents representative blots for insulin signaling protein analysis.

JNK activation has been implicated in HFD-induced insulin resistance. Figure 6a presents representative blots for JNK activation. JNK activation was greater in HFD groups compared with LFD controls (LFD Sham versus HFD Sham, $p = 0.001$; LFD PBM versus HFD PBM, $p = 0.00003$). However, the HFD PBM group showed lower JNK activation in comparison with the HFD SHAM group ($p = 0.005$) (Fig. 6b).

Sample size

Statistical power and effect size regarding epididymal adipocyte area among all groups were calculated in order to ensure the minimal power of 80%, alpha (α) of 5%, and large effect size (greater than 0.75). We used the mean of epididymal adipocyte area of each group and the highest value of standard deviation among all groups. For epididymal adipocyte area, our results demonstrate a difference between groups with a statistical power of 89%, effect size of 1.09 (very large effect size), and total sample size of 16, i.e., 4 animals per group (4 groups). These calculations demonstrate that sample size, power, and effect size of this study were considered to be satisfactory.

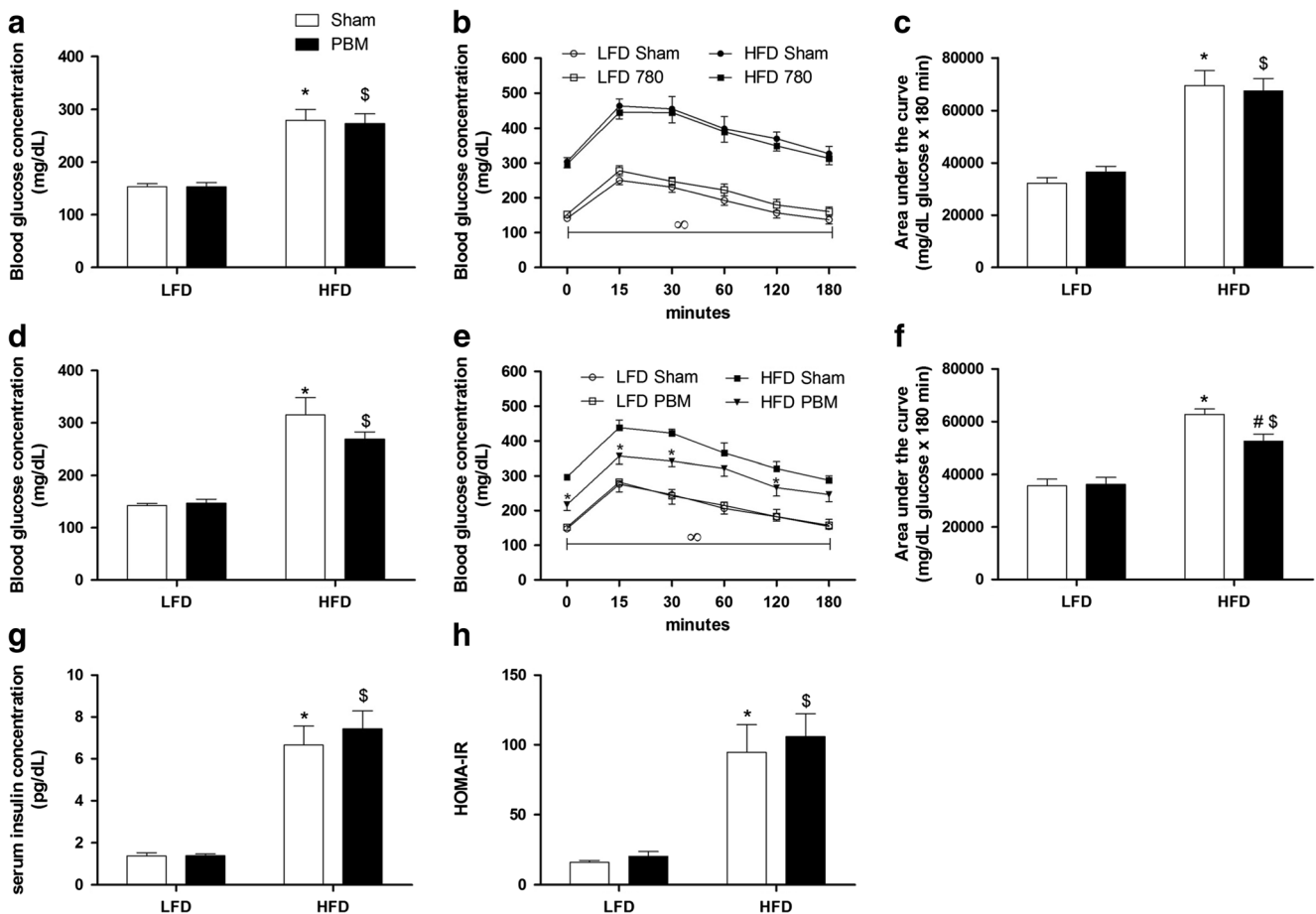


Fig. 4 Effect of low-fat diet (LFD) or high-fat diet (HFD) for 8 weeks on **a** blood glucose concentration, **b** glucose tolerance, and **c** area under the curve (AUC); and effect of LFD or HFD for 12 weeks and photobiomodulation during the last 4 weeks of diet on **d** blood glucose concentration, **e** glucose tolerance, **f** area under the curve (AUC), **g** serum

insulin concentration, and **h** homeostatic model assessment of insulin resistance (HOMA-IR). * $p < 0.05$ versus LFD Sham; \$ $p < 0.05$ versus LFD PBM; # $p < 0.05$ versus HFD Sham; ∞ $p < 0.05$ LFD groups versus HFD groups

Discussion

To our best knowledge, the present study is the first to investigate the effects of PBM therapy on HFD-induced obesity and insulin resistance and cellular signaling in mice. The main findings were PBM therapy in HFD mice (a) lower increases in epididymal fat pad mass and epididymal and mesenteric adipocyte area; (b) reduced total serum cholesterol concentration; (c) improved glucose intolerance; (d) preserved intracellular insulin pathway activation and GLUT4 content in epididymal fat; (e) attenuated JNK activation in epididymal fat. Altogether, these results suggest that PBM may be a useful therapy to treat deleterious effects of HFD-induced fat accumulation and lipid and glucose metabolism.

It has been demonstrated that HFD induces fat gain in rodents [19]. Importantly, visceral fat pad mass was greater in HFD Sham mice. Visceral fat accumulation has been implicated in the development of metabolic alterations that can lead to cardiovascular and metabolic diseases, as insulin resistance, T2D, and metabolic syndrome [20]. In the present

study, we showed that PBM therapy inhibited HFD-induced increase in epididymal and mesenteric adipocyte area and epididymal fat pad mass. Aquino et al. [21] observed that PBM therapy using infrared laser (830 nm; 100 mW) applied to the lower hind limbs combined with physical exercise reduced retroperitoneal and epididymal fat pad weight in rats, although sedentary animals treated with LLLT did not show reduction in fat pad mass. In the present study, the PBM therapy was applied on the ventral region of the animals targeting the fat pad directly, which may explain the differences in the results of these studies. On the other hand, Aquino et al. [22] observed that the infrared laser reduced visceral adipocyte area in HFD-treated rats, but again, in that study, only the lower hind limbs were targeted (two points; 4.7 J/per point), which might have attenuated the observed effects of PBM therapy on adipocyte area reduction.

Total serum cholesterol and serum triglyceride concentration were not altered by HFD in the present study. These results are in accordance with White et al. [23] which did not observe dyslipidemia in HFD-fed Swiss mice treated for

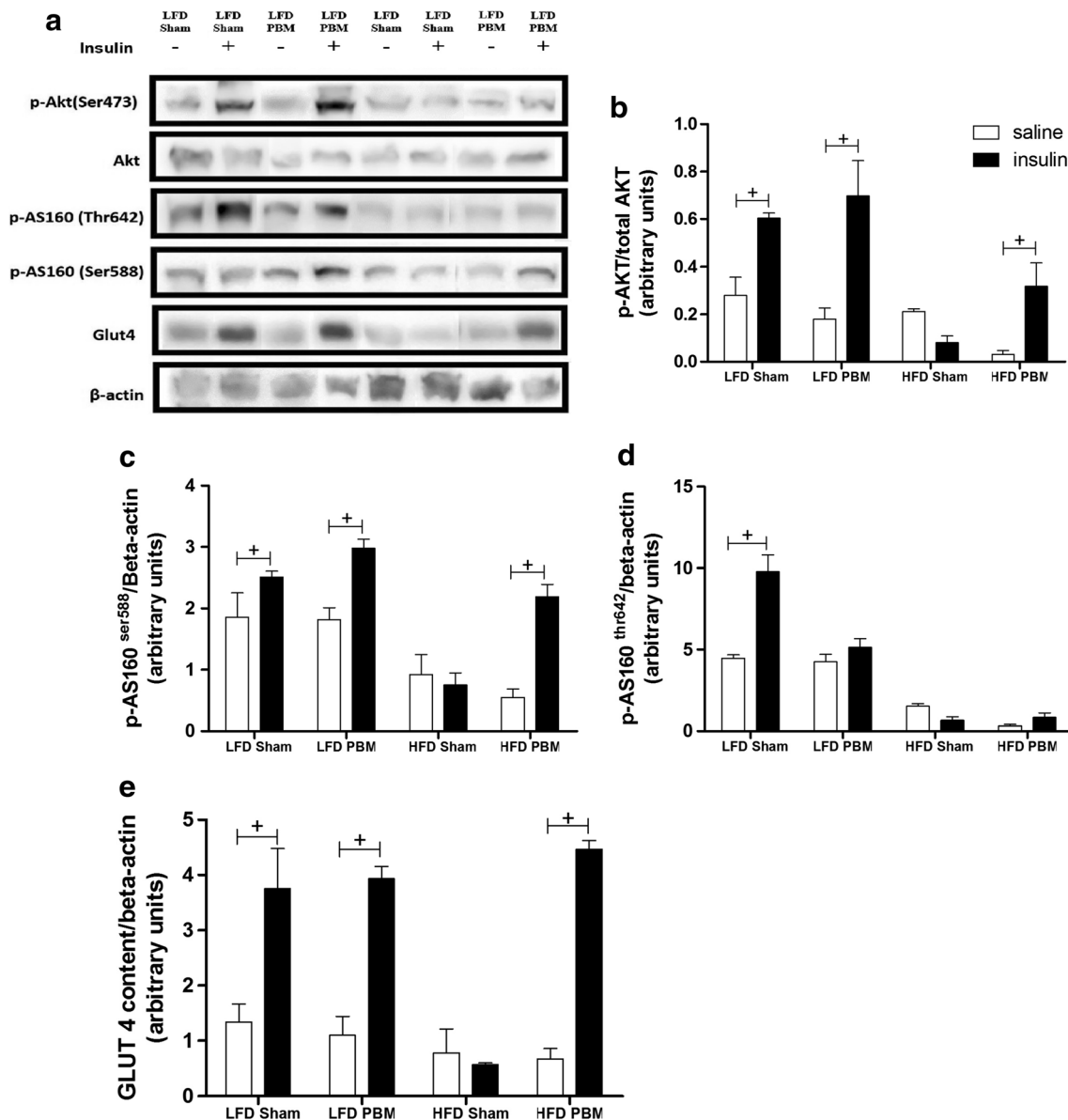


Fig. 5 Effect of photobiomodulation (PBM) and insulin stimulation on insulin signaling in low-fat diet (LFD)-fed and high-fat diet (HFD)-fed mice. **a** Representative blots and quantification of **b** AKT

phosphorylation, **c** AS160 ser588 phosphorylation, **d** AS160 thr642 phosphorylation, and **e** GLUT4 content. + $p < 0.05$ for insulin effect

10 weeks. Interestingly, however, our results showed that in HFD PBM-treated mice, total serum cholesterol concentration was reduced. In Aquino et al. [21], a reduction of total cholesterol and triglyceride concentration in HFD-treated rats was observed in response to the laser (830 nm). These results suggest that PBM may be a useful therapy to treat dyslipidemia, although more researches on that area are certainly necessary.

In the present study, PBM therapy did not alter HFD-induced increase in fasting hyperglycemia, hyperinsulinemia, and insulin resistance, as assessed by HOMA-IR. On the other hand, PBM therapy improved glucose intolerance in HFD-fed mice. These results might be explained by the fact that fasting measurements, such as HOMA-IR, are more related to hepatic

insulin resistance, while ipGTT reflects peripheral as well as hepatic insulin resistance [24]. Therefore, the present results suggest that PBM therapy may likely have produced effects on peripheral tissues, such as skeletal muscles and adipose tissue (sites of PBM irradiations in this study) while the liver was not exposed and/or affected by the PBM therapy. To the best of our knowledge, there are no data or studies reporting the isolated effect of PBM on glucose metabolism. However, the effects of aerobic physical exercise and photobiomodulation were investigated by Sene-Fiorese et al. [14] in obese women. Those authors observed that the combination of physical exercise and PBM therapy was more effective in reducing circulating insulin concentration and HOMA-IR index than exercise

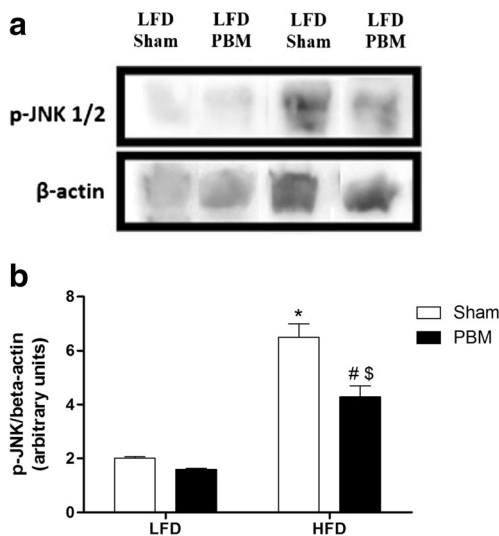


Fig. 6 Effect of photobiomodulation (PBM) on JNK activation in low-fat diet (LFD)-fed and high-fat diet (HFD)-fed mice. **a** Representative blots and **b** quantification of JNK activation. * $p < 0.05$ versus LFD Sham; \$ $p < 0.05$ versus LFD PBM, # $p < 0.05$ versus HFD Sham

alone. Therefore, these preliminary results suggest that PBM therapy may be used mainly in combination with physical exercise to improve glucose metabolism.

This is the first study to investigate the effects of PBM therapy on the insulin signaling pathway. Briefly, insulin signaling involves insulin binding to its receptor on the plasmalemma, and the phosphorylation of insulin receptor substrates, which in turn is responsible for the phosphorylation of phosphatidylinositol 3-kinase, and activates Akt. Akt acts on its substrate, AS160, to allow the trafficking and anchoring of GLUT4 to the cell membrane to allow glucose uptake [25]. AS160 function is regulated by serine and threonine residue phosphorylation in response to insulin or muscle contraction [26]. More than 10 residues have been described in AS160 [27], and among them, thr642 and ser588 seem to be the key residues in mediating GLUT4 translocation in response to insulin stimulus [28]. In the present study, the phosphorylation of some components of this pathway was assessed: AKT (ser473), AS160 (thr642) and AS160 (ser588) and GLUT4 content in epididymal fat. The epididymal fat is one of the visceral adipose tissues commonly associated with the development of insulin resistance in mice [29]. It has been repeatedly shown that HFD and/or obesity lead to decrease—insulin signaling activation [30]. Our results showed that PBM therapy diminished HFD-induced reductions in insulin activation mediated by AKT, AS160 (ser588) phosphorylation, and GLUT4 content. Similarly, other studies have described alteration in AS160 thr642 and ser588 in insulin resistance. Consitt et al. [31] observed that reduced insulin action in humans was associated with

reduced AS160 phosphorylation in ser588, thr642, and ser666, and regression analysis showed that body fat percentage was the best predictor of ser588 phosphorylation and of the insulin plasma levels of thr642, suggesting different regulations to each site.

Increased Akt and AS160 phosphorylation leadS to GLUT4 translocation and increased expression [32]. The results of this study demonstrated that PBM therapy prevented HFD-induced decrease in GLUT4 content. In this context, PBM therapy seems to exert similar effects to physical exercise, which is considered one of the most important non-pharmacological strategies to prevent and treat insulin resistance and T2D. Physical exercise is known to increase insulin sensitivity, which is associated with greater Akt activation, phosphorylation of its downstream substrates and, consequently, increased translocation and expression of GLUT4 [33].

Previous studies have demonstrated the role of MAPKs in the development of insulin resistance [9]. The JNK seems to be one of the most important MAPKs implicated in this condition in HFD mice [10]. It was observed in the present study that PBM therapy attenuated HFD-induced increase in JNK activation. These results agree with Chung et al. [34] that reported higher JNK activation in skeletal muscle of insulin-resistant individuals compared with healthy individuals. We are unaware of any studies that have investigated the effects of PBM therapy on JNK activation; therefore, our study is the first to report that PBM therapy can reduce JNK activation in the context of insulin resistance.

It has been shown that HFD-induced insulin resistance is related to mitochondrial dysfunction [35, 36]. Mitochondrial dysfunction has been suggested to result in activation of several serine and/or threonine kinases leading to serine phosphorylation of IRS-1 and thus compromising insulin signaling [7, 36]. Further, previous studies have already reported that the effects of PBM therapy are related to the stimulation of mitochondrial function through enhanced cytochrome c oxidase activity, a key enzyme in the electron transport chain [37, 38]. In this context, the wavelength (780 nm) chosen was based on its better tissue penetration compared to short wavelengths (examples: blue [~480 nm] and green [~530 nm]), and also due to the optical window, which reports that wavelengths from 650 to 1200 nm have less absorption by tissue chromophores as hemoglobin and melanin [39]. Moreover, a previous critical review already pointed that wavelengths ranging from 760 to 895 nm can be absorbed by cytochrome c oxidase, mainly by its binuclear copper centers (Cu_A , Cu_B), and then promote stimulation of mitochondrial function [37]. We speculate that the observed effects of PBM therapy on HFD-induced insulin resistance and signaling may be mediated by modulation of mitochondrial retrograde signaling [40]. Improved mitochondrial function can lead to decreased lipid intermediate accumulation (i.e., as diacylglycerol, fatty

acyl-CoA, and ceramides) and lower JNK activation, thus may result in enhanced insulining signaling pathway activation.

In conclusion, infrared PBM therapy (780 nm) promoted beneficial effects on fat accumulation and glucose metabolism, as well as in the insulin signaling in HFD-fed mice. These beneficial effects seem to be related to the PBM therapy effects on adipocyte hypertrophy and reductions in JNK activation, leading to an improved insulin pathway activation. Thus, our findings suggest that PBM therapy may represent a potential therapeutic resource to treat insulin resistance. Finally, as a limitation of this study, the therapeutic window for light dose was not investigated.

Acknowledgments The authors disclose receipt of financial support for the research, authorship, and/or publication of this article: CAPES (PNPD-2455/2011), FAPEMIG (APQ-01915-13 and APQ-03058-16), and CNPq (447007/2014-9) grants. The authors wish to acknowledge Kurt A. Escobar for reviewing the manuscript. The authors would like to acknowledge the Centro Integrado de Pós-Graduação e Pesquisa em Saúde at the Universidade Federal dos Vales do Jequitinhonha e Mucuri, Diamantina, MG, for providing equipments and technical support for experiments.

Compliance with ethical standards All procedures followed the National Council of Animal Experimentation (Brazil) and were approved by the local Ethics Committee on Animal Use under the number 028/2014.

Conflict of interest The authors declare that they have no conflict of interest.

References

- Lewis CE, McTigue KM, Burke LE, Poirier P, Eckel RH, Howard BV, Allison DB, Kumanyika S, Pi-Sunyer FX (2009) Mortality, health outcomes, and body mass index in the overweight range: a science advisory from the American Heart Association. *Circulation* 119(25):3263–3271. <https://doi.org/10.1161/CIRCULATIONAHA.109.192574>
- Eikenberg JD, Davy BM (2013) Prediabetes: a prevalent and treatable, but often unrecognized, clinical condition. *J Acad Nutr Diet* 113(2):213–218. <https://doi.org/10.1016/j.jand.2012.10.018>
- Rui L (2013) Brain regulation of energy balance and body weight. *Rev Endocr Metab Disord* 14(4):387–407. <https://doi.org/10.1007/s11154-013-9261-9>
- Samuel VT, Shulman GI (2016) The pathogenesis of insulin resistance: integrating signaling pathways and substrate flux. *J Clin Invest* 126(1):12–22. <https://doi.org/10.1172/JCI77812>
- Havens L, Danielsson KN, Fogelstrand L, Wiklund O (2009) Induction of proinflammatory cytokines by long-chain saturated fatty acids in human macrophages. *Atherosclerosis* 202(2):382–393. <https://doi.org/10.1016/j.atherosclerosis.2008.05.033>
- Trayhurn P, Wood IS (2004) Adipokines: inflammation and the pleiotropic role of white adipose tissue. *Br J Nutr* 92(3):347–355
- Hirabara SM, Curi R, Maeckler P (2010) Saturated fatty acid-induced insulin resistance is associated with mitochondrial dysfunction in skeletal muscle cells. *J Cell Physiol* 222(1):187–194. <https://doi.org/10.1002/jcp.21936>
- Hage Hassan R, Pacheco de Sousa AC, Mahfouz R, Hainault I, Blachnio-Zabielska A, Bourron O, Koskas F, Gorski J, Ferre P, Fougelle F, Hajdouch E (2016) Sustained action of ceramide on THE insulin signaling pathway in muscle cells: IMPLICATION OF THE DOUBLE-STRANDED RNA-ACTIVATED PROTEIN KINASE. *J Biol Chem* 291(6):3019–3029. <https://doi.org/10.1074/jbc.M115.686949>
- Fujishiro M, Gotoh Y, Katagiri H, Sakoda H, Ogihara T, Anai M, Onishi Y, Ono H, Abe M, Shojima N, Fukushima Y, Kikuchi M, Oka Y, Asano T (2003) Three mitogen-activated protein kinases inhibit insulin signaling by different mechanisms in 3T3-L1 adipocytes. *Mol Endocrinol* 17(3):487–497. <https://doi.org/10.1210/me.2002-0131>
- Hirosumi J, Tuncman G, Chang L, Gorgun CZ, Uysal KT, Maeda K, Karin M, Hotamisligil GS (2002) A central role for JNK in obesity and insulin resistance. *Nature* 420(6913):333–336. <https://doi.org/10.1038/nature01137>
- Braverman B, McCarthy RJ, Ivankovich AD, Forde DE, Overfield M, Bapna MS (1989) Effect of helium-neon and infrared laser irradiation on wound healing in rabbits. *Lasers Surg Med* 9(1):50–58
- Liang HL, Whelan HT, Eells JT, Meng H, Buchmann E, Lerch-Gaggl A, Wong-Riley M (2006) Photobiomodulation partially rescues visual cortical neurons from cyanide-induced apoptosis. *Neuroscience* 139(2):639–649. <https://doi.org/10.1016/j.neuroscience.2005.12.047>
- Begum R, Powner MB, Hudson N, Hogg C, Jeffery G (2013) Treatment with 670 nm light up regulates cytochrome C oxidase expression and reduces inflammation in an age-related macular degeneration model. *PLoS One* 8(2):e57828. <https://doi.org/10.1371/journal.pone.0057828>
- Sene-Fiorese M, Duarte FO, de Aquino Junior AE, Campos RM, Masquio DC, Tock L, de Oliveira Duarte AC, Damaso AR, Parizotto NA, Bagnato VS (2015) The potential of phototherapy to reduce body fat, insulin resistance and "metabolic inflexibility" related to obesity in women undergoing weight loss treatment. *Lasers Surg Med* 47(8):634–642. <https://doi.org/10.1002/lsm.22395>
- Matthews DR, Hosker JP, Rudenski AS, Naylor BA, Treacher DF, Turner RC (1985) Homeostasis model assessment: insulin resistance and beta-cell function from fasting plasma glucose and insulin concentrations in man. *Diabetologia* 28(7):412–419
- de Matos MA, Ottone Vde O, Duarte TC, Sampaio PF, Costa KB, Fonseca CA, Neves MP, Schneider SM, Moseley P, Coimbra CC, Magalhaes Fde C, Rocha-Vieira E, Amorim FT (2014) Exercise reduces cellular stress related to skeletal muscle insulin resistance. *Cell Stress Chaperones* 19(2):263–270. <https://doi.org/10.1007/s12192-013-0453-8>
- Aguiar PF, Magalhaes SM, Fonseca IA, da Costa Santos VB, de Matos MA, Peixoto MF, Nakamura FY, Crandall C, Araujo HN, Silveira LR, Rocha-Vieira E, de Castro Magalhaes F, Amorim FT (2016) Post-exercise cold water immersion does not alter high intensity interval training-induced exercise performance and Hsp72 responses, but enhances mitochondrial markers. *Cell Stress Chaperones* 21(5):793–804. <https://doi.org/10.1007/s12192-016-0704-6>
- Bradford MM (1976) A rapid and sensitive method for the quantitation of microgram quantities of protein utilizing the principle of protein-dye binding. *Anal Biochem* 72:248–254
- Schmid GM, Converset V, Walter N, Sennitt MV, Leung KY, Byers H, Ward M, Hochstrasser DF, Cawthorne MA, Sanchez JC (2004) Effect of high-fat diet on the expression of proteins in muscle, adipose tissues, and liver of C57BL/6 mice. *Proteomics* 4(8):2270–2282. <https://doi.org/10.1002/pmic.200300810>
- Zhang M, Hu T, Zhang S, Zhou L (2015) Associations of different adipose tissue depots with insulin resistance: a systematic review and meta-analysis of observational studies. *Sci Rep* 5:18495. <https://doi.org/10.1038/srep18495>
- Aquino AE Jr, Sene-Fiorese M, Paolillo FR, Duarte FO, Oishi JC, Pena AA Jr, Duarte AC, Hamblin MR, Bagnato VS, Parizotto NA

- (2013) Low-level laser therapy (LLLT) combined with swimming training improved the lipid profile in rats fed with high-fat diet. *Lasers Med Sci* 28(5):1271–1280. <https://doi.org/10.1007/s10103-012-1223-z>
22. Aquino AE Jr, Sene-Fiorese M, Castro CA, Duarte FO, Oishi JC, Santos GC, Silva KA, Fabrizzi F, Moraes G, Matheus SM, Duarte AC, Bagnato VS, Parizotto NA (2015) Can low-level laser therapy when associated to exercise decrease adipocyte area? *J Photochem Photobiol B* 149:21–26. <https://doi.org/10.1016/j.jphotobiol.2015.04.033>
 23. White PA, Cercato LM, Araujo JM, Souza LA, Soares AF, Barbosa AP, Neto JM, Marcal AC, Machado UF, Camargo EA, Santos MR, Brito LC (2013) Model of high-fat diet-induced obesity associated to insulin resistance and glucose intolerance. *Arq Bras Endocrinol Metabol* 57(5):339–345
 24. Singh B, Saxena A (2010) Surrogate markers of insulin resistance: a review. *World J Diabetes* 1(2):36–47. <https://doi.org/10.4239/wjd.v1.i2.36>
 25. Saltiel AR, Kahn CR (2001) Insulin signalling and the regulation of glucose and lipid metabolism. *Nature* 414(6865):799–806. <https://doi.org/10.1038/414799a>
 26. Treebak JT, Pehmoller C, Kristensen JM, Kjobsted R, Birk JB, Schjerling P, Richter EA, Goodyear LJ, Wojtaszewski JF (2014) Acute exercise and physiological insulin induce distinct phosphorylation signatures on TBC1D1 and TBC1D4 proteins in human skeletal muscle. *J Physiol* 592(2):351–375. <https://doi.org/10.1113/jphysiol.2013.266338>
 27. Sakamoto K, Holman GD (2008) Emerging role for AS160/TBC1D4 and TBC1D1 in the regulation of GLUT4 traffic. *Am J Phys Endocrinol Metab* 295(1):E29–E37. <https://doi.org/10.1152/ajpendo.90331.2008>
 28. Sharma N, Wang H, Arias EB, Castorena CM, Cartee GD (2015) Mechanisms for independent and combined effects of calorie restriction and acute exercise on insulin-stimulated glucose uptake by skeletal muscle of old rats. *Am J Phys Endocrinol Metab* 308(7):E603–E612. <https://doi.org/10.1152/ajpendo.00618.2014>
 29. Lee BC, Kim MS, Pae M, Yamamoto Y, Eberle D, Shimada T, Kamei N, Park HS, Sasorith S, Woo JR, You J, Mosher W, Brady HJ, Shoelson SE, Lee J (2016) Adipose natural killer cells regulate adipose tissue macrophages to promote insulin resistance in obesity. *Cell Metab* 23(4):685–698. <https://doi.org/10.1016/j.cmet.2016.03.002>
 30. Wiedemann MS, Wueest S, Item F, Schoenle EJ, Konrad D (2013) Adipose tissue inflammation contributes to short-term high-fat diet-induced hepatic insulin resistance. *Am J Phys Endocrinol Metab* 305(3):E388–E395. <https://doi.org/10.1152/ajpendo.00179.2013>
 31. Consitt LA, Bell JA, Houmard JA (2009) Intramuscular lipid metabolism, insulin action, and obesity. *IUBMB Life* 61(1):47–55. <https://doi.org/10.1002/iub.142>
 32. Hawley JA, Lessard SJ (2008) Exercise training-induced improvements in insulin action. *Acta Physiol* 192(1):127–135. <https://doi.org/10.1111/j.1748-1716.2007.01783.x>
 33. Frosig C, Rose AJ, Treebak JT, Kiens B, Richter EA, Wojtaszewski JF (2007) Effects of endurance exercise training on insulin signaling in human skeletal muscle: interactions at the level of phosphatidylinositol 3-kinase, Akt, and AS160. *Diabetes* 56(8):2093–2102. <https://doi.org/10.2337/db06-1698>
 34. Chung J, Nguyen AK, Henstridge DC, Holmes AG, Chan MH, Mesa JL, Lancaster GI, Southgate RJ, Bruce CR, Duffy SJ, Horvath I, Mestrl R, Watt MJ, Hooper PL, Kingwell BA, Vigh L, Hevener A, Febbraio MA (2008) HSP72 protects against obesity-induced insulin resistance. *Proc Natl Acad Sci U S A* 105(5):1739–1744. <https://doi.org/10.1073/pnas.0705799105>
 35. Choo HJ, Kim JH, Kwon OB, Lee CS, Mun JY, Han SS, Yoon YS, Yoon G, Choi KM, Ko YG (2006) Mitochondria are impaired in the adipocytes of type 2 diabetic mice. *Diabetologia* 49(4):784–791. <https://doi.org/10.1007/s00125-006-0170-2>
 36. Martins AR, Nachbar RT, Gorjao R, Vinolo MA, Festuccia WT, Lambertucci RH, Cury-Boaventura MF, Silveira LR, Curi R, Hirabara SM (2012) Mechanisms underlying skeletal muscle insulin resistance induced by fatty acids: importance of the mitochondrial function. *Lipids Health Dis* 11:30. <https://doi.org/10.1186/1476-511X-11-30>
 37. Karu TI (2010) Multiple roles of cytochrome c oxidase in mammalian cells under action of red and IR-A radiation. *IUBMB Life* 62(8):607–610. <https://doi.org/10.1002/iub.359>
 38. Avci P, Nyame TT, Gupta GK, Sadasivam M, Hamblin MR (2013) Low-level laser therapy for fat layer reduction: a comprehensive review. *Lasers Surg Med* 45(6):349–357. <https://doi.org/10.1002/lsm.22153>
 39. Huang YY, Chen AC, Carroll JD, Hamblin MR (2009) Biphasic dose response in low level light therapy. *Dose Response* 7(4):358–383. <https://doi.org/10.2203/dose-response.09-027.Hamblin>
 40. Gao X, Xing D (2009) Molecular mechanisms of cell proliferation induced by low power laser irradiation. *J Biomed Sci* 16:4. <https://doi.org/10.1186/1423-0127-16-4>